Article

Integrating Geospatial Techniques for Urban Land Use Classification in the Developing Sub-Saharan African City of Lusaka, Zambia

Matamyo Simwanda * and Yuji Murayama

Faculty of Life and Environmental Sciences, University of Tsukuba, 1-1-1 Tennodai, Tsukuba City, Ibaraki 305-8572, Japan; mura@geoenv.tsukuba.ac.jp
* Correspondence: matamyo@gmail.com; Tel.: +81-701-255-2705

Abstract: For most sub-Saharan African (SSA) cities, in order to control the historically unplanned urban growth and stimulate sustainable future urban development, there is a need for accurate identification of the past and present urban land use (ULU). However, studies addressing ULU classification in SSA cities are lacking. In this study, we developed an integrated approach of remote sensing and Geographical Information System (GIS) techniques to classify ULU in the developing SSA city of Lusaka. First, we defined six ULU classes (i.e., unplanned high density residential; unplanned low density residential; planned medium-high density residential; planned low density residential; commercial and industrial; public institutions and service areas). ULU parcels, created using road networks as homogenous units separating ULU classes, were used to classify ULU. We utilised the combined detail of cadastral and land use data plus high-resolution Google Earth imagery to infer ULU and classify the parcels. For residential ULU, we also created density thresholds for accurate separation of the classes. We then used the classified ULU parcels for post-classification sorting of built-up pixels extracted from three Landsat TM/ETM+ imageries (1990, 2000, and 2010) into respective ULU classes. Three ULU maps were produced with overall accuracy values of 84.09% to 85.86%. The maps provide information that is relevant to urban planners and policy makers for sustainable future urban planning of Lusaka City. The study also provides an insight for ULU classification in SSA cities with complex urban landscapes similar to Lusaka.

Keywords: urban land use; remote sensing; GIS; parcels; ancillary data; Sub-Saharan Africa

1. Introduction

Urban land use (ULU) classification, i.e., discriminating the built-up-area into different ULU types (e.g., residential, industrial, commercial, public, etc.) remains a challenge in remote sensing urban studies due to spectral confusion among ULU classes within the urban environment [1]. The complexity and heterogeneity of urban environments is a major contributing factor to this problem [2]. The problem is especially apparent in sub-Saharan African (SSA) cities due to their highly complex mix of spatial structures and spectral confusion resulting from the wide range of construction material used to build the structures [3]. While it is more appealing to attribute the ULU classification problems to inadequate imagery spatial resolution, it is, however, mostly caused by the limitations of the commonly used imagery classification techniques (e.g., pixel-based classification) [4]. In fact, inconsistent recommendations are regularly made on the choice of classification techniques, despite many studies using different types of imagery data with varying spatial resolutions [5].

To overcome this problem, several studies have attempted to develop different approaches that integrate remote sensing data with additional data or analysis. Nonetheless, most of the methods

developed have limited applicability for various reasons. Some studies use imagery with high spatial resolution [6–8] that are not often available or too expensive, particularly in developing countries (e.g., SSA countries). Other studies use ancillary data, such as geographical data [9,10] and census data [11,12], which is also either not available or inconsistent with remote sensing data in most SSA cities. Additionally, the variations in the level of complexity of urban land use/cover (LUC) among different localities limits most methods from being applied under a different set of conditions [5]. For example, most of the noted improvements in urban land use/cover classification using advanced classification techniques have been conducted in developed countries, which are characterised by a highly developed urban built-up environment and well-planned ULU system [13,14]. On the other hand, SSA cities are characterised by urban environments with a complex mix of ULUs, usually displaying chaotic spatial patterns dominated by unplanned/informal settlements haphazardly located close to urban growth centres, such as the Central Business District and commercial and industrial areas. The chaotic spatial structures and resulting spectral mix-up among different ULUs in SSA cities presents additional challenges to applying advanced methods, such as those that incorporate structure information [2,15–17] and texture features [6,18].

Therefore, there is still a need to explore approaches for ULU classification that can work at local and regional scales, particularly in urban cities in developing regions like SSA. Moreover, despite ULU classification being an important issue in the remote sensing literature [12] and detailed ULU information being important to urban planners and policy makers [19], very few urban studies have addressed ULU in SSA cities. Actually, most of the urban studies using remote sensing and GIS techniques in SSA consider all ULUs as one individual category, often referred to as built-up land (e.g., [13,14,20].) The broad simplification of different ULU types into one class severely limits information that is essential for urban development planning. Most SSA cities are in urgent need of ULU policies and plans that can drive the reconstruction, control, and upgrade of the historically unplanned urban growth and stimulate desired future urban development. Detailed information on the spatial distribution of different ULUs can help the planning authorities in SSA cities to decide on the appropriate infrastructure development and provision of social services, especially in unplanned areas. Therefore, accurate identification of the past and present ULU is imperative. This means there is need for SSA urban studies to consider classifying the built-up urban area into different ULU classes.

Lusaka, like most SSA cities, has been experiencing rapid uncontrolled and unplanned urban growth. Consequently, Lusaka's urban landscape has become complex with a chaotic mix of ULUs including unplanned informal settlements that are haphazardly located close to the Central Business District, and commercial and industrial areas. To control the historically unplanned urban growth and stimulate sustainable future urban development, there is need for accurate identification of the past and present ULU in Lusaka. Therefore, the primary objective of this study was to classify the ULU of the developing SSA city of Lusaka, Zambia, over time (1990–2010) using remote sensing and Geographical Information System (GIS) techniques. To the best of our knowledge, no study has produced ULU classification maps for the city of Lusaka. In view of the inherent challenges of ULU classification, including the complexity of SSA urban settings and the resulting spectral confusion among ULU types, the limited availability and cost of high-resolution remote sensing data, and the limited applicability of available ULU classification methods, we developed a framework integrating remote sensing and GIS techniques to classify ULU. Our approach involved the integration of freely available remote sensing data sets (i.e., medium-resolution Landsat TM/+ETM and high resolution Google Earth imagery) with spatial ancillary data, including detailed road networks, cadastral polygons, and land use data. Based on our expert knowledge of the study area, we defined six ULU classes (i.e., unplanned high density residential; unplanned low density residential; planned medium-high density residential; planned low density residential; commercial and industrial; public institutions and service areas). In this study, we describe the details of the proposed approach used to classify ULU in Lusaka City, as well as its issues and limitations. We conclude with a discussion on the importance of the results obtained to urban development planning and give recommendations for future research.

2. Study Area and Data

2.1. Study Area

The city of Lusaka is situated in the Lusaka Province of Zambia and is the provincial headquarters as well as the country's capital city (Figure 1). Its central geographical coordinates are 15° 24′ 24″ S and 28° 17′ 13″ E, with an administrative area covering approximately 420 km². Lusaka is also the political, cultural, and economic centre of the country and home of the central government. As such, many institutional, commercial, and industrial activities are concentrated in Lusaka. The city has a population of approximately 2 million and dominates the urban system in Zambia. The city of Lusaka has the largest share (79.3%) of the urban population in Lusaka Province, which it shares with three other districts, and it accounts for 32% of the total urban population of the country [21]. Like other SSA cities, the urban built-up land in Lusaka is characterised by a complex mix of ULU categories, including planned and unplanned residential areas, plus others such as commercial, industrial, and institutional ULU.
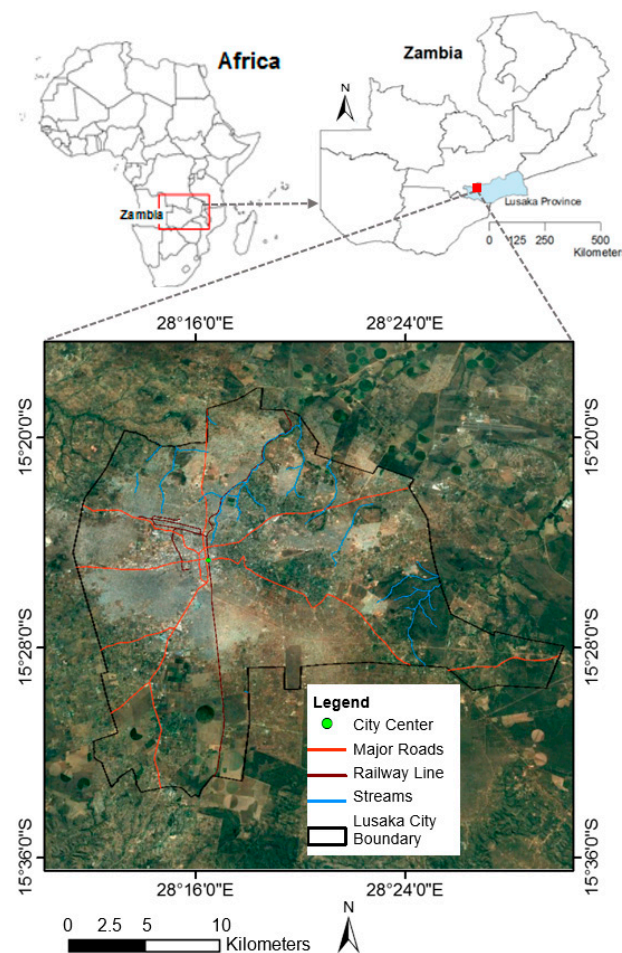
Figure 1. Location map of the city of Lusaka, showing the city centre, major roads, railway line, streams, and the current administrative city boundary.

2.2. Data

In this study, multi-temporal medium-resolution remote sensing satellite imageries were obtained from the US Geological Survey website (http://earthexplorer.usgs.gov/) and used to extract the LUC information for Lusaka city. We downloaded three imageries (path 172/row 71): two Landsat-5 TM imageries acquired on the 21st of June 1990 and the 27th of May 2010, respectively, and one Landsat-7

ETM+ imagery acquired on the 5th of April 2000. The spatial resolution of all the imageries was 30 m. For optimal ULU classification, care was taken to ensure that the imageries were cloud free (<10%) and acquired within the same season. High-resolution Google Earth imagery was also used as reference data in this study.

Ancillary spatial data were also collected to aid in ULU classification. The main ancillary spatial data collected included detailed cadastral and land use data, as well as road network data for the city of Lusaka. Cadastral and land use data were obtained from the local planning authority, the Lusaka City Council, while the road networks data were obtained from the Road Development Agency of Zambia. Other reference data obtained from the Lusaka City Council that was used for reference included the latest city administrative boundary, a 1985 topographic map (scale 1:50,000), a 2003 partial QuickBird satellite imagery (0.6 m spatial resolution), and the Lusaka urban development plan (2010–2030).

3. Methods

The framework illustrating the whole approach developed in this study for ULU classification is shown in Figure 2. Our approach included two major steps: (1) LUC classification and built area extraction and (2) ULU classification as described in the sections hereunder.

3.1. LUC Classification and Built Area Extraction

In our approach, the first critical step was to accurately extract the built-up area before dividing it into different ULU classes. Therefore, a thorough LUC classification approach was adopted. We developed a classification scheme comprising six separate classes: built-up, cropland, grassland, bare land, woodland, and water. LUC classification using the six LUC classes was conducted to detect any spectral confusion between the built-up class and any of the other five classes, thereby ensuring that the built-up area was accurately extracted. A combination of pixel-based and object-based classification techniques, plus post-classification image control, was employed to produce LUC maps from the Landsat TM/ETM+ imageries (Figure 2-1a–m). Several studies have shown the advantages of combining pixel-based and object-based classification techniques to overcome their individual limitations and produce more accurate LUC maps [22–24].

3.1.1. Pixel-Based Classification

In this study, we first applied the supervised maximum likelihood pixel-based classification (PBC) technique to process the Landsat imageries in ArcGIS (version 10.2) (Figure 2-1a–f). Training sites were selected for each of the six LUC classes by identifying representative features on the ground using different spectral band combinations together with reference to the ancillary data. Ten to fifteen training sample sites, with sizes ranging from 88 to 723 pixels, were created for each LUC class. However, misclassifications were observed among some of the LUC classes due to spectral confusions emanating from the complex and heterogeneous nature of the study area. The major problem was the confusion between agricultural areas and other vegetation classes, especially grasslands, due to spectral similarities. There was also confusion between bare land and agriculture areas with no crop cover. In other instances, the built-up area was over or under estimated due to the spectral mix-up in the informal/unplanned settlement areas. The spectral mix-up in these areas could be attributed to the wide range of construction material used to build the structures [3]. However, we ensured that an acceptable level of accuracy in the LUC maps was attained before using the other methods to deal with the errors from PBC.

3.1.2. Object-Based Classification

In our second step, we applied an object-based classification (OBC) technique to control the errors from PBC (Figure 2-1a,g–i). In the OBC approach, we segmented the Landsat imageries into separate image objects using the multi-resolution segmentation algorithm in eCognition Developer software (version 9) [25]. The segmentation process in eCognition software uses three parameters, namely scale,

shape, and compactness that are assigned by the user to determine the shape and maximum size of the resulting homogeneous image objects. The shape and compactness control the homogeneity based on spectral information and overall compactness of image objects, respectively, while the scale determines the maximum size of image objects [25]. The user iteratively runs the process while changing the values of the three parameters until image objects are attained that visually correspond to features on the ground. Image segmentation was performed at three scales (5, 15, 40) with constant values of shape (0.1) and compactness (0.5) to produce image objects with different sizes for each Landsat imagery. Smaller scale parameters were used to capture ground features with fine and medium scales in the study area, such as small-scale farming fields with no crop cover and some informal built-up areas. The larger image scale parameter was used to identify larger objects on the ground (e.g., large scale agriculture). Small segments representing the same LUC classes were then merged. Each of the three scale image objects produced were exported as shapefiles for post-classification image control in ArcGIS.

3.1.3. Post-Classification

Post-classification image control was used to improve the accuracy of the PBC results by integrating ancillary spatial data [9] and visual interpretation of misclassified areas [26] with the OBC image segments (Figure 2-1j). The ancillary spatial data used for this purpose included Google Earth imagery, the 1985 topographic map, and the 2003 partial QuickBird imagery. An overlay process of the object-based image segments, ancillary spatial data, and the initial PBC-LUC maps was carried out, together with visual interpretation, to determine the misclassified areas. The object-based image segments representing different LUC classes were used to clip out misclassified pixels, which were then reclassified into the correct classes and mosaicked back to replace all incorrectly classified pixels. For the purpose of this study all LUC classes were then merged into one class (i.e., non-built-up) except the built-up and water classes. Finally, we produced three LUC maps for 1990, 2000, and 2010 with three categories (built-up, non-built-up, and water) (Figure 2-1l). The built-up class was then extracted for ULU classification (Figure 2-1m).

3.1.4. LUC Classification Accuracy Assessment

To assess the accuracy with which the built-up area was extracted (Figure 2-1k), 300 stratified random points were generated for the three LUC maps. Stratification was chosen to ensure that each of the two LUC classes (built-up and non-built-up) had 150 random points allocated to them. Randomisation in point selection reduced bias [27]. All the random points were taken to represent ground truth data and were visually assessed using Google Earth, topographic maps, and the author's vast local knowledge of the study area. Data based on the comparisons between reference points and actual points on the LUC maps was used to calculate the overall accuracy of the LUC maps [27].
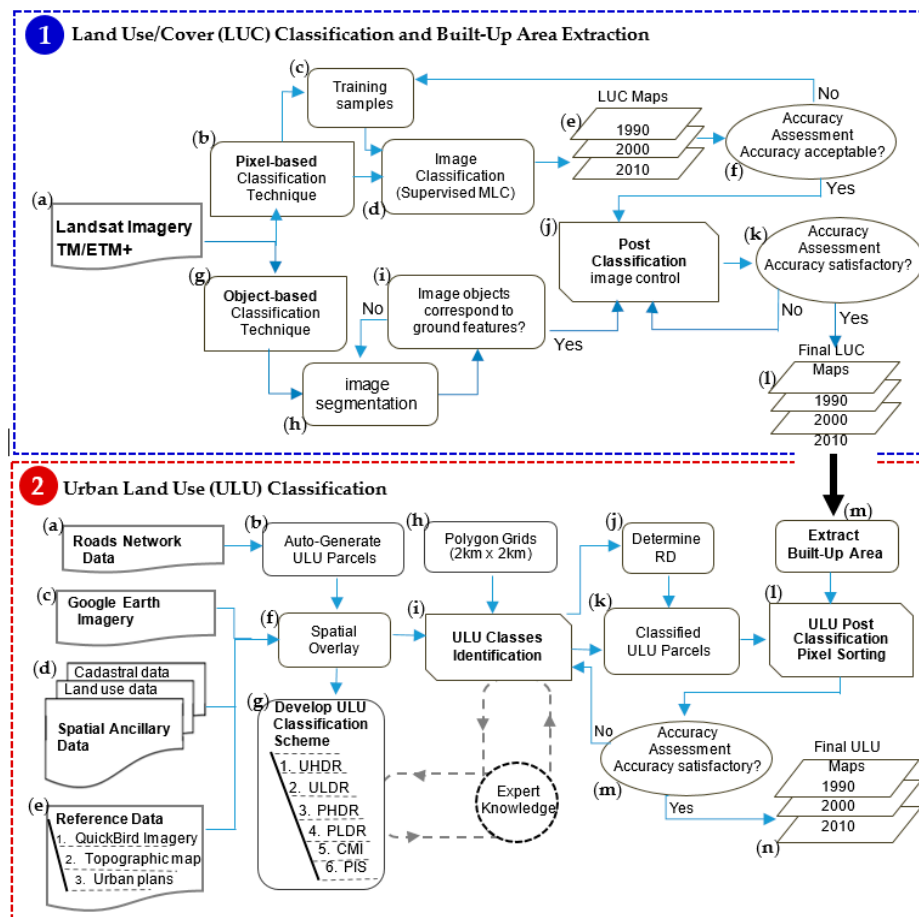
3.2. ULU Classification

ULU classification (i.e., separation of the built-up-area into different ULU categories) remains a challenge, especially in regions in the developing world, like in SSA countries. One approach that has shown significant improvements in ULU classification accuracy at local or regional scales is referred to as the expert system approach [28–30]. Expert systems allow for the integration of remotely sensed data with other sources of geo-referenced information (e.g., ancillary land use data) to obtain greater classification accuracy [28]. In this approach, the experts define logical decision rules that are used with the various datasets to carry out post-classification sorting of pixels into different urban LUC classes from the initial classification [28]. The main strengths of expert-based approaches are their flexibility to data sources and the potential for application to different research questions [30].

In this study, we developed a somewhat expert-based ULU classification approach using the built-up pixels extracted from medium-resolution Landsat TM/+ETM data (Section 3.1 above), road networks data, detailed cadastral and land use spatial data, Google Earth imagery, and expert

knowledge of the study area (Figure 2-2). In brief, the study area was first delineated into ULU parcels using the road networks data based on the method proposed by [31] and later used by [10] (Figure 2-2a,b). We defined ULU parcels as polygon units separated by roads serving as natural segmentation boundaries of the urban area with relatively homogeneous ULU classes [10,31]. After creating the ULU parcels, we separated, merged, or refined the parcels based on their homogeneity with respect to the six ULU classes as defined in our classification scheme, shown in Table 1 below. ULU classes were identified using the detailed cadastral and land use data and expert-based visual interpretation of high-resolution Google Earth imagery (Figure 2-2b–j). We produced polygon coverage of ULU parcels for the entire study area, representing the six ULU classes (Figure 2-2k). We then carried out post-classification sorting of built-up pixels into their respective ULU classes using the final ULU parcels (Figure 2-2k). After validating a hypothesis of no transitions among ULU classes (e.g., residential to commercial and vice versa), we used the same ULU parcels to sort built-up pixels for each of the three time points (1990, 2000, and 2010) in this study, since ULU was inferred based on the latest date (2010). Finally, we produced three ULU maps and carried out accuracy assessment, along with validating our hypothesis (Figure 2-2m–n). Our ULU classification approach is described in detail in the following sections.

Figure 2. Proposed framework for classifying urban land use (ULU): (1) a–m shows the order of the steps for urban land use/cover (LUC) classification and built area extraction and (2) a–n shows the order of the steps for ULU classification. MLC refers to maximum likelihood classification. RD refers to residential density. UHDR, ULDR, PMHDR, PLDR, CMI, and PIS refer to Unplanned High Density Residential, Unplanned Low Density Residential, Planned Medium-High Density Residential, Planned Low Density Residential, Commercial and Industrial, and Public Institutions and Service, respectively.

3.2.1. Classification Scheme

Six ULU classes were defined based on the detailed cadastral and land use spatial data, our expert knowledge of the study area, and consultations with experts from the local planning office. Table 1 gives the descriptions of the six ULU classes. Figure 3 also shows examples of ULU classes from Google Earth imagery.

Table 1. Description of urban land use classes.

Urban Land Use Class	Code	Description
Unplanned High Density Residential	UHDR	Residential areas (RD^1 > 2,000 du/km^2) comprising informal/slum/squatter settlements with many small houses located close to each other showing an enormously unsystematic spatial arrangement. Average RD was estimated at 5000 du/km^2 and PD^2 at 12,000–28,000 people/km^2
Unplanned[3] Low Density Residential	ULDR	Residential areas (RD ≤ 2000 du/km^2) comprising medium sized houses with slightly big lot sizes but showing a relatively unsystematic spatial arrangement. Average RD was estimated at 1500 du/km^2 and PD at 400–2000 people/km^2
Planned[4] Medium-High Density Residential	PHMDR	Residential areas (RD > 2000 du/km^2) with many small and medium sized houses located close to each other showing a systematic spatial arrangement. Average RD was estimated at 3000 du/km^2 and PD at 2000–22,000 people/km^2
Planned Low Density Residential	PLDR	Residential areas (RD ≤ 2000 du/km^2) comprising large houses with big lot sizes and showing a systematic spatial arrangement. Average RD was estimated at 1000 du/km^2 and PD at 400–2000 people/km^2
Commercial and Industrial	CMI	Commercial: General retail, shopping malls, markets, hotels, financial services (banks), roads, rails, etc.Industrial: Manufacturing, warehousing, quarrying, mining facilities, and commercial agriculture facilities
Public Institutions and Service	PIS	Areas comprising education and health facilities, religious institutions, government and administration houses, municipal utilities, transportation terminals, aviation facilities, etc.
Non-Built-Up	NBU	All vegetated areas (forest and grassland), bare lands, and agriculture areas
Water	WT	Rivers, streams, dams, etc.

Note: [1] RD is residential density, which refers to the intensity with which land is occupied by housing development measured in dwelling units (du) per square kilometres (km^2). [2] PD is population density, which is estimated based on the aggregated ward level 2010 population census data for Lusaka [21]. [3] Unplanned refers to all illegal/informal/slum/squatter settlements and all other areas that developed without proper authorisation, as declared by local planning office. These areas lack basic services and are mainly characterised by unpaved roads and no connection to the municipal water and sanitation services. [4] Planned refers to all areas that developed with proper authorisation from the local planning office. These areas generally have all basic services, including paved roads and municipal water and sanitation services.
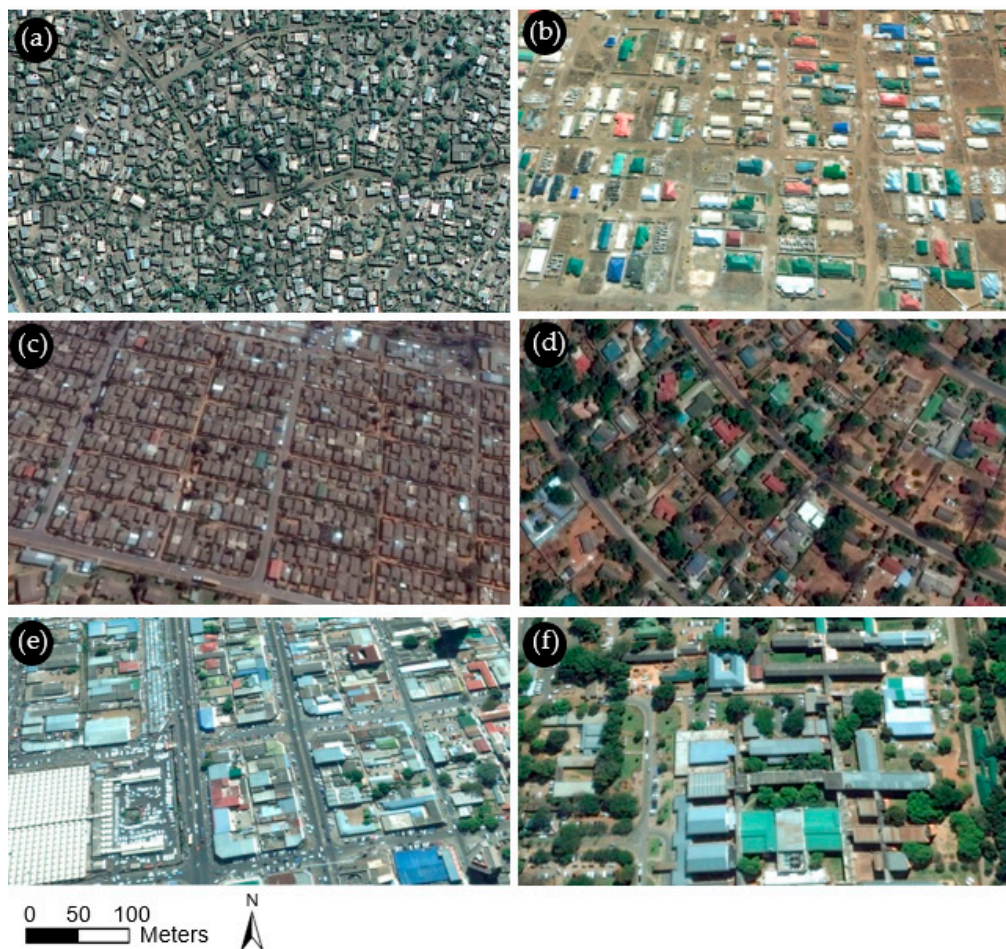
Figure 3. Examples of urban land use classes from Google Earth imagery (Date: 13 June 2011): (**a**) UHDR; (**b**) ULDR; (**c**) PHMDR; (**d**) PLDR; (**e**) CMI; and (**f**) PIS.

3.2.2. Creating ULU Parcels

A working definition of a parcel from [31] was adopted and we defined a parcel as a polygon containing a single ULU class, segmented by roads as its boundaries. Before creating the parcels, the road network data was prepared using GIS to clean out all short (<200 m) and hanging roads to avoid the confusion of many small parcels and hanging polylines. All the road polylines were also buffered to widths ranging from 5 m to 20 m, depending on road class. The road network in the city of Lusaka is divided into main, district, urban, and feeder roads with standards widths of 9.1, 8.5, 6.1, and 5.5 m, respectively. Thus, as an example, a dual carriage main road was buffered to 20 m. After preparing the road network data, the ULU parcels were then automatically generated in GIS by merging and connecting all road segments (Figure 2a,b and Figure 4b). ULU parcels were taken as the spaces between roads, while road spaces were taken as a separate ULU sub-class. We obtained a total of 4197 parcels.

3.2.3. Identification of ULU Classes

To start with, it is important to note that we did not use any additional spectral information derived from the study area for ULU identification. This was mainly due to high spectral mix-up between ULU classes in the study area. The high spectral complexity made it impossible to develop any indices or thresholds that would separate the ULU classes based on additional spectral information, such as structure and texture, like other expert systems [2,28,29].
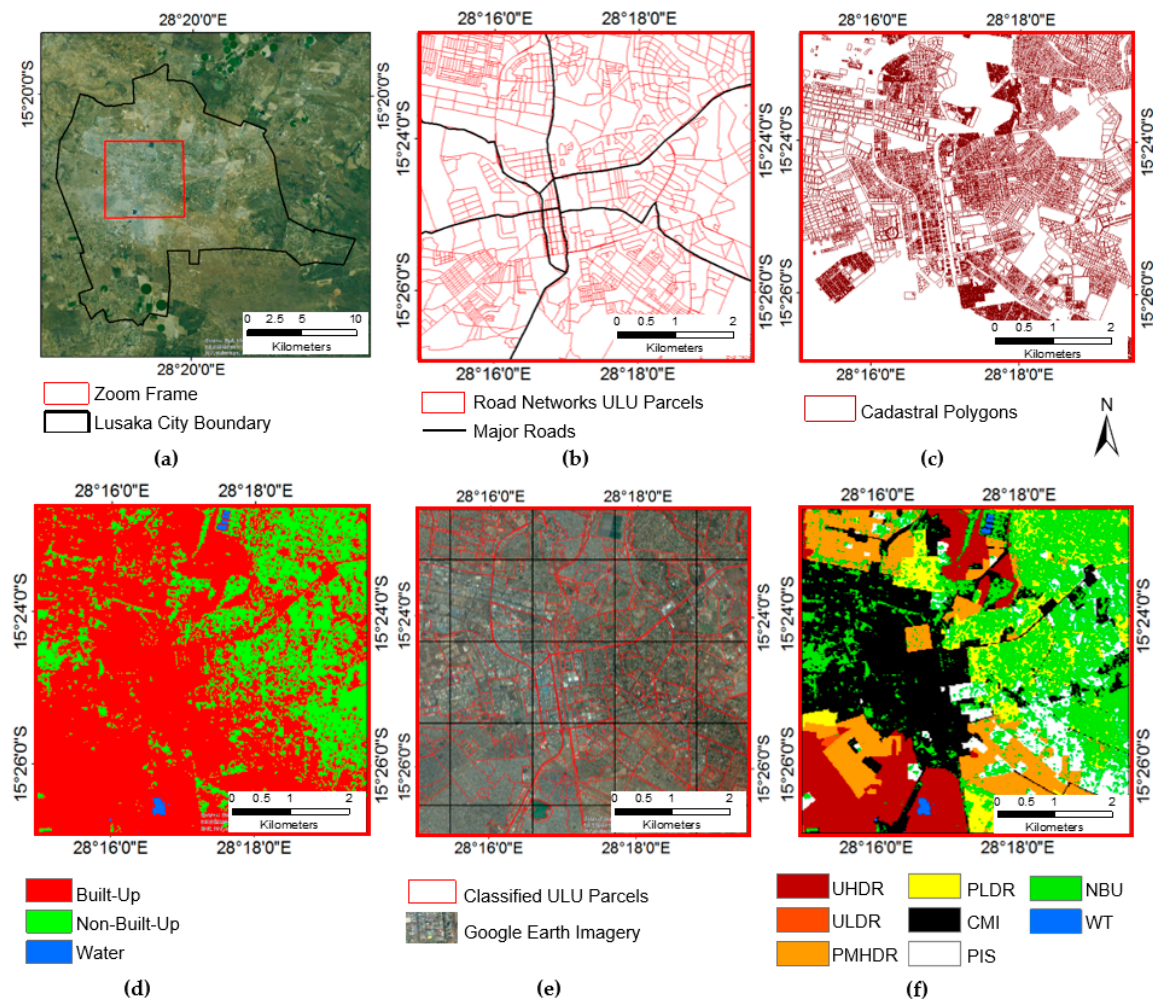
Figure 4. ULU identification: (**a**) shows the study area boundary and zoom frame; (**b**) zoomed in view of road networks ULU parcels; (**c**) cadastral polygons; (**d**) LUC classification results; (**e**) final classified ULU parcels; and (**f**) post-classification pixel sorting ULU results.

Instead, we used the detailed information from cadastral and land use data, as well as expert visual interpretation of high-resolution Google Earth imagery, to infer ULU and give parcels identities based on their homogeneity with respect to the six ULU classes defined in Table 1 (Figure 2-2). Figure 4 shows examples of the data and results from the ULU identification process. The cadastral data was provided in the form of a spatial catalogue of polygons with names or codes for the city area sub-divisions, as well as the physical delineation of land and property boundaries in these areas (Figure 4c). Cadastral data also indicated the unplanned and planned areas of Lusaka. The combined detail of cadastral and land use data included detailed location information of the different ULU types: unplanned and planned residential areas (low-, medium-, and high-density); commercial areas (general retail, shops, markets, hotels etc.); industrial areas (e.g., manufacturing plants, quarrying facilities, warehouses, etc.); recreation facilities (sports centres, parks, etc.); as well as other public institutions and service areas (education and health facilities, religious institutions, government and administration houses). Reference was also made to the urban development and land use plan (2010–2030), as it contained detailed information on the existing ULU at the plan date (2008). The plan was obtained in vector format.

To identify ULU, first all ULU parcels were overlaid, together with cadastral and land use and all other reference data, with high-resolution Google Earth imagery. (Figure 2-2b–f). Then, the detailed information of ULU attributes from the cadastral and land use data was aggregated into the six

ULU classes. For example, all general retail, markets, manufacturing plants, and warehouses were placed under the CMI class. All education and health facilities were placed under the PIS class. Next, we automatically assigned ULU attributes of the six ULU classes to parcels. We then applied expert visual interpretation of high-resolution Google Earth imagery, while closely referring to the cadastral and land use data, as well as the urban development and land use plan, to scrutinise the homogeneity of the ULU parcels. All homogenous and non-homogeneous ULU parcels were then identified. Adjacent homogenous ULU parcels falling within one ULU class were further merged. For example, if several parcels representing the CMI ULU class were found within the same area, these parcels were aggregated into one large ULU parcel. Non-homogenous ULU parcels were also refined. If an ULU parcel contained more than one ULU class or the physical delineation of one or more classes was not clear, we applied expert-based on-screen digitisation to ensure homogeneity among ULU parcels. Expert-based on-screen digitisation of parcels was mostly useful in unplanned areas, as they lacked clear road networks. Worth noting is that expert knowledge of the study area played a crucial role, especially in cases where there were similarities between two ULU classes (e.g., between unplanned and planned high-density residential areas). Thus, for residential ULU classes, we also calculated the residential density to create thresholds and further separate the classes based on our classification scheme (see Section 3.2.4). To ensure that ULU for the entire study area was covered and to reduce the potential for human error, we adopted a systematic approach by creating 224 grid polygons (2 km × 2 km) that were also overlaid with all the other data (Figure 2h and 4e). ULU classes within parcels were systematically identified by carefully going through each grid from 1 to 224. Finally, we ended up with 1989 classified ULU parcels representing the six ULU classes defined in this study (Figures 2l–n and 4e).

3.2.4. Determining Residential Density

While the residential ULU classes were identified through their spatial characteristics and by using the cadastral and land use data, to accurately separate the classes based on our classification scheme, we created thresholds by estimating the residential density (RD). RD in Lusaka is regulated by the number of housing units allowed per unit area. Accordingly, housing units in areas with low RD are allocated lager lot sizes than areas with high RD. Thus, high RD areas have more housing units per unit area. Therefore, we defined RD as the intensity with which land is occupied by housing development measured in dwelling units (du) per unit area of a parcel in square kilometre (km^2).

Equation (1) was used to determine the RD of each residential parcel:

$$RD_i = \frac{\sum DU_i}{PA_i} \tag{1}$$

where RDi is the RD in the *i*th residential parcel, DUi is a dwelling unit in the *i*th residential parcel, and PAi is the total area of the ith residential parcel in km^2.

Equation (2) was used to determine the average RD for each ULU class:

$$ARD_c = \frac{\sum_{i=1}^{n} RD_i}{N} \tag{2}$$

where ARDc is the average RD of each residential ULU class and *N* (or *n*) is the total number of parcels in each residential ULU class.

To decide on the appropriate RD thresholds, we first checked the maximum and minimum lot sizes of dwelling units in low, medium, and high RD areas using the cadastral polygons. We determined that, generally, the lot sizes in low RD areas are greater than 500 m^2, while those in the medium and high RD areas are less than 500 m^2. This means that the RD of medium and high RD areas in Lusaka is generally greater than 2000 du/km^2 and vice versa. After estimating the RD for all residential parcels, we separated the classes as follows. Residential parcels under unplanned areas with RD > 2000 du/km^2 were classified as UHDR and those parcels with RD ≤ 2000 du/km^2 were classified

as ULDR. The ARD*c* in UHDR and PLDR is about 5000 du/km^2 and 1500 du/km^2, respectively. Residential parcels under planned areas with RD > 2000 du/km^2 were classified as PMHDR. The ARD*c* in PMHDR is about 3000 du/km^2. Accordingly, planned areas with residential parcels with RD ≤ 2000 du/km^2 were classified as PLDR with ARD*c* of about 1000 du/km^2.

3.2.5. Post-Classification Pixel Sorting

After classifying all the parcels, we overlaid the ULU parcels with the extracted built-up pixels from the initial LUC classification described in Section 3.1 above. We used the classified parcels to carry out post-classification sorting of the built-up pixels into ULU classes (Figures 2k and 4d–f). To do this, we extracted the built-up pixels for each ULU class using the classified parcels representing that class. We then reclassified all the built-up pixels and identified them with their respective ULU class. All reclassified built-up pixels were then merged together with the non-built-up and water classes to produce ULU maps comprising the six ULU classes and the non-built-up and water classes.

In this study, ULU within parcels was inferred based on the latest date (2010). To produce ULU maps for the three time points (1990, 2000, and 2010), we hypothesised that there were no transitions among ULU classes (e.g., residential to commercial and vice versa). This hypothesis meant that built-up pixels representing a certain ULU class in 2010 would still represent the same ULU class in the preceding years (2000 and 1990) if it existed or otherwise represented the non-built-up class. For example, built-up pixels representing a commercial building in 2010 would still represent a commercial building in 2000 and 1990, if it existed in those years, otherwise it would be non-built-up. Therefore, the same classified parcels would qualify to be used for reclassifying the built-up pixels into their respective ULU classes in each of the three time points. Our aim was not only to produce one ULU map for the latest date (2010) but to also produce ULU maps for 1990 and 2000. The objective was to provide information that can be used for assessing the current situation in ULU, as well as trend analysis by urban planners and policy makers. Hence, three ULU maps for 1990, 2000, and 2010 were produced and we then proceeded to perform an accuracy assessment and validate our hypothesis.

3.2.6. Accuracy Assessment and Hypothesis Validation

To assess the performance of the ULU classification approach, a second accuracy assessment exercise was conducted. We could not verify the accuracy of the ULU map for 1990 due to the absence of Google Earth imagery for that time. However, since the ULU for the study was inferred based on the data from 2010, verifying the accuracy of the ULU maps for 2000 and 2010 was taken to be representative of the overall performance of our proposed approach. In addition, an initial accuracy assessment of the LUC maps to confirm the accuracy with which the built-up area was extracted had already been conducted (see Section 3.1.4). We generated 679 and 509 random points for the years 2000 and 2010, respectively, and examined all the points using high-resolution Google Earth imagery as the ground truth reference. The random points created for 2010 were also used to validate our hypothesis by checking if ULU classes were the same for each point in 2010 and 2000, or at least non-built-up in 2000. The Google Earth imagery used had capture dates close to or at the same time as the ULU Maps (i.e., 2000 and 2010). For the year 2000, we also used the 2003 Quickbird imagery for accuracy assessment. The reference points were then compared with actual points for the two ULU maps and the data obtained was used to calculate the accuracies of the ULU classes.

Based on [27], we created an error matrix for each ULU map and determined the producer and user accuracies for each ULU class, as well as the overall accuracy and kappa statistics for both the 2000 and 2010 ULU maps. The producer and user accuracies (P_A and U_A) were computed based on Equations (3) and (4), respectively.

$$P_A = \frac{X_{ii}}{X_{i+}} \times 100 \tag{3}$$

$$U_A = \frac{X_{ii}}{X_{+i}} \times 100 \tag{4}$$

where X_{ii} is the number of correct ULU points in row *i* and column *i* and X_{i+} and X_{+i} are the marginal totals of row *i* and column *i*, respectively.

Equations (5) and (6) were used to calculate the overall accuracies (O_A) and kappa statistics (*K*), respectively.

$$O_A = \frac{\sum_{i=1}^{r} X_{ii}}{N} \times 100 \tag{5}$$

$$\hat{K} = \frac{N \sum_{i=1}^{r} X_{ii} - \sum_{i=1}^{r} X_{i+} \times X_{+i}}{N^2 - \sum_{i=1}^{r} X_{i+} \times X_{+i}} \tag{6}$$

where *r* is the number of ULU classes in the matrix and *N* is the total number of points used in the accuracy assessment exercise.

4. Results

4.1. LUC Classification and Built-Area Extraction

Figure 5 presents the LUC classification maps of Lusaka for 1990, 2000, and 2010 with three classes: built-up, non-built-up, and water. The accuracy assessment results for the three LUC classification maps revealed overall accuracy values of 89.2%, 91.3%, and 93.0% for 1990, 2000, and 2010, respectively. All the overall accuracies recorded exceeded the minimum standard of 85% recommended by [32]. These accuracy results indicated that the built-up class was accurately identified and extracted, which was one of the critical steps in our ULU classification approach. These accuracies were partly achieved by merging all non-built-up LUC classes (i.e., forest, grassland, cropland, and bare land) into one class, which reduced the likelihood of error [33], aside from combining more than one geospatial technique (i.e., PBC, OBC, and post-classification techniques) to carry out LUC classification.
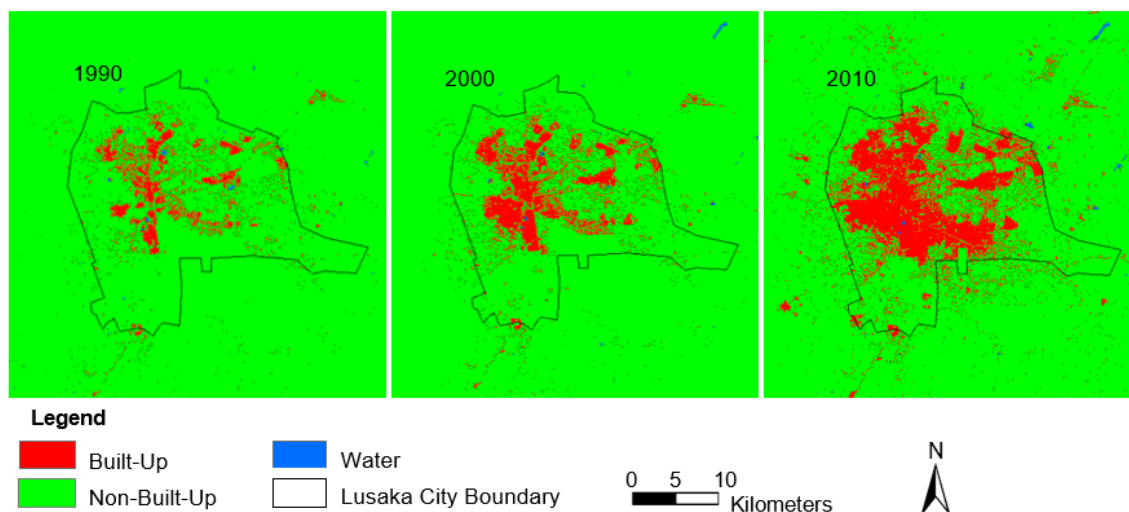

Figure 5. LUC classification maps of Lusaka for 1990, 2000, and 2010.

4.2. ULU Classification

4.2.1. Accuracy Assessment and Hypothesis Validation

As stated earlier, during ULU classification we advanced an assumption that built-up pixels representing an ULU class in 2010 would represent the same ULU class in the preceding years (2000 and 1990) if it existed, or otherwise represent the non-built-up class in 2000. The hypothesis validation exercise revealed that our hypothesis was valid, as 98% of the 679 points checked were either the same ULU class in both 2010 and 2000, or at least non-built-up in the year 2000. This result approved the hypothesis that there were no transitions among ULU classes (e.g., residential to commercial and vice

versa) and further affirmed the concept of using the same defined ULU parcel to classify ULU at each of the three time points (1990, 2000, and 2010), provided that ULU was inferred based on the latest date (2010). The production of three ULU maps using our proposed approach was therefore validated.

Table 2 presents the error matrix and accuracy assessment results for the years 2000 and 2010. The accuracy assessment results show that the 2010 ULU map had an overall classification accuracy of 84.09%, with a kappa coefficient of 80.63%. The 2000 ULU map had a slightly higher accuracy with an overall classification accuracy of 85.86% and a kappa coefficient of 84.02%. The overall accuracy values and kappa statistics achieved were sufficiently high (>80%) and therefore considered to be acceptable. In terms of individual ULU classes, for the 2010 ULU map the CMI class had the highest producer accuracy (95.49%) followed by PIS (89.36%), UHDR (88.15%), and ULDR (80.60%). The PMHDR and PLDR classes had comparatively lower producer accuracy values (73.88% and 72.41%, respectively). For the 2000 ULU map, the CMI, PIS, and UHDR classes had the highest producer accuracy values (92.39%, 89.66%, and 88.30%, respectively). The other classes with high producer accuracy values were PMHDR (84.09%) and PLDR (81.16%). ULDR class had the lowest producer accuracy (74.29%). The errors in both the 2010 and 2000 ULU maps generally resulted from confusion among residential ULU classes, especially between PMHDR and UHDR. Relatively few errors resulted from confusion between low-density residential land uses and the CMI and PIS classes. Nonetheless, all accuracy values recorded were sufficiently high and considered to represent ULU in the study area.

Table 2. Error matrix and accuracy of ULU maps (2010 and 2000).

ULU Map	Classified Data	Reference Data						Total	UA (%)
		UHDR	ULDR	PMHDR	PLDR	CMI	PIS		
2010	UHDR	186	0	17	0	0	0	203	91.63
	ULDR	4	54	10	4	0	1	73	73.97
	PMHDR	21	5	99	11	0	2	138	71.74
	PLDR	0	8	8	63	1	0	80	78.75
	CMI	0	0	0	3	127	2	132	96.21
	PIS	0	0	0	6	5	42	53	79.25
	Total	211	67	134	87	133	47	679	
	PA (%)	88.15	80.60	73.88	72.41	95.49	89.36		
	Overall Classification Accuracy = 84.09%, Overall Kappa Coefficient = 80.63%								
2000	UHDR	151	4	7	1	0	0	163	92.64
	ULDR	2	26	0	0	0	0	28	92.86
	PMHDR	18	5	112	4	0	0	139	80.58
	PLDR	0	0	9	37	4	2	52	71.15
	CMI	0	0	5	0	85	1	91	93.41
	PIS	0	0	5	2	3	26	36	72.22
	Total	171	35	138	44	92	29	509	
	PA (%)	88.30	74.29	81.16	84.09	92.39	89.66		
	Overall Classification Accuracy = 85.86%, Overall Kappa Coefficient = 84.02%								

Note: UA represents user's accuracy and PA represents producer's accuracy.

4.2.2. ULU Maps and Statistics

The final ULU maps produced are presented in Figure 6 and Table 3 presents the statistics of the ULU classification results. According to the statistics, the total ULU area increased from 49.17 km^2 in 1990, to 84.17 km^2 in 2000, and 158.81 km^2 in 2010, thus representing 12%, 20%, and 38% of the total study area, respectively. Two residential land use classes, namely UHDR and PMHDR, as well as the CMI class dominate ULU from 1990 to 2010. From the total study area, UHDR constituted 13.85 km^2 (3.32%) in 1990, 25.26 km^2 (6.05%) in 2000, and 46.88 km^2 (11.22%) in 2010; PMHDR constituted 14.18 km^2 (3.40%) in 1990, 21.96 km^2 (5.26%) in 2000, and 32.17 km^2 (7.7%) in 2010; and

CMI constituted 11.2 km^2 (2.68%) in 1990, 19.31 km^2 (4.62%) in 2000, and 33.65 km^2 (8.06%) in 2010. The statistics also indicate that low-density residential land uses (i.e., ULDR and PLDR) and PIS areas were relatively very small at each of the three time points. The area classified as ULDR was only 0.99 km^2 (0.24%) in 1990, 2.31 km^2 (0.55%) in 2000, and significantly increased to 15.89 km^2 (3.80%) in 2010. PLDR accounted for only 4.77 km^2 (1.14%) in 1990, 9.00 km^2 (2.16%) in 2000, and 20.61 km^2 (4.93%) in 2010. The area classified as PIS accounted for only 4.18 km^2 (1.0%), 6.32 km^2 (1.51%), and 9.61 km^2 (2.30%) in 1990, 2000, and 2010, respectively. The non-built-up area decreased from 87.95% to 61.88% of the total study area between 1990 and 2010. The area occupied by water was relatively very small and also decreased from 0.28% to 0.10% between 1990 and 2010.
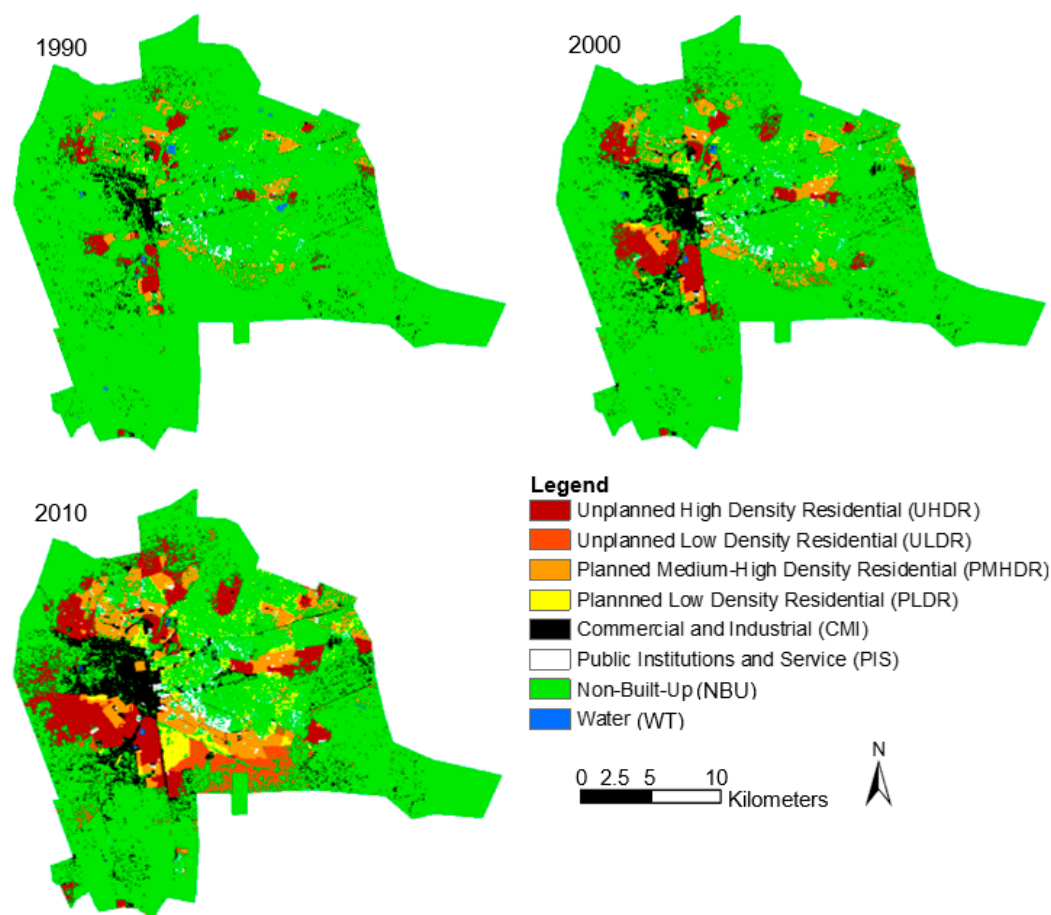

Figure 6. Urban land use maps of Lusaka for 1990, 2000, and 2010.

Table 3. ULU classification statistics.

ULU Class	1990		2000		2010	
	Area (Km^2)	%	Area (Km^2)	%	Area (Km^2)	%
UHDR	13.85	3.32	25.26	6.05	46.88	11.22
ULDR	0.99	0.24	2.31	0.55	15.89	3.80
PMHDR	14.18	3.40	21.96	5.26	32.17	7.70
PLDR	4.77	1.14	9.00	2.16	20.61	4.93
CMI	11.20	2.68	19.31	4.62	33.65	8.06
PIS	4.18	1.00	6.32	1.51	9.61	2.30
NBU	367.36	87.95	333.11	79.75	258.47	61.88
WT	1.16	0.28	0.52	0.12	0.41	0.10
Total	418	100	418	100	418	100

5. Discussion

5.1. Performance of ULU Classification Approach

In this study, we employed an integrated framework of remote sensing and GIS techniques to classify ULU in the city of Lusaka. We developed a somewhat expert-based ULU classification approach by integrating freely available remote sensing data sets (i.e., medium-resolution Landsat TM/+ETM and high resolution Google Earth imagery) with spatial ancillary data, including detailed road networks, cadastral polygons, and land use data. In our approach, the first critical step was to accurately extract the built-up area from Landsat imagery. We applied a combination of pixel-based and object-based classification techniques plus post-classification image control to produce LUC maps with high overall classification accuracies (89.2%–93.0%), thereby accurately extracting the built-up area. Other studies have combined these LUC classification techniques and reported similar high overall classification accuracies [22–24]. To classify ULU, we used ULU parcels created by using the road network data as homogenous polygon subdivisions separating the ULU classes in the study area. The use of parcels created using road network data was previously tested and proven to be an effective approach for identifying and separating ULU [10,31]. We also utilised ancillary data (i.e., cadastral and land use data) containing detailed information of ULU attributes alongside expert-based visual interpretation of high-resolution Google Earth imagery to accurately identify ULU classes in the study area. Previous studies have also identified the usefulness of integrating remote sensing and other types of ancillary data in urban LUC classification. Some of the ancillary data used in the literature include: zoning and housing density data [9]; population census data [11,12]; municipal master plan [34]; social media data [35]; and geographical points of interest data [10,35]. Some recent studies have also explored and recommended using high-resolution Google Earth imagery for improved LUC classification through visual interpretation [36–39]. To produce ULU maps for the three time points (1990, 2000, and 2010), we hypothesised that there were no transitions among ULU classes, meaning built-up pixels representing a certain ULU class in 2010 would be the same class in the preceding years (2000 and 1990) if it existed, or at least represent the non-built-up class. This hypothesis qualified the same classified ULU parcels to be used for reclassifying the built-up pixels into their respective ULU classes at each of the three time points, provided ULU was inferred based on the latest date (2010). Our validation results revealed that our hypothesis was valid for the study area, with 98% of the checked points supporting the hypothesis. The overall classification accuracy values (84.09% and 85.86%) and kappa coefficients (80.63% and 84.02%) of ULU maps are within the same range as previous studies that classified ULU [10,12,40].

Therefore, this study is a contribution to the current efforts of ULU classification, which has remained one of the hot issues in remote sensing urban studies. To the best of our knowledge, this study is the first of its kind in the study area and one of the very few studies that have attempted to classify ULU in the complex urban settings of SSA cities. In view of the inherent challenges of ULU classification, including the complexity of SSA urban areas and the resulting spectral confusion among ULU types, the limited availability and cost of high-resolution remote sensing data, as well as the limited applicability of available ULU classification methods, this study demonstrates that ULU classification can be achieved by integrating a mix of geospatial techniques. This study has shown that through utilising more than one geospatial technique and additional ancillary spatial data (e.g., road network, cadastral, and land use data), the challenges and limitations encountered when using freely available remote sensing datasets (i.e., Landsat and Google Earth imagery) can be overcome to an acceptable level. Another key success of our approach is the production of ULU maps for more than one time point, which is dissimilar to previous ULU studies [10,12,40]. The ULU maps produced in this study provide detailed information on the spatial-temporal patterns of ULU in the study area of Lusaka. In addition, the statistics provide insight into the trends of ULU in Lusaka. This information can help urban planners and policy makers, including other concerned stakeholders (e.g., researchers), to analyse the city growth and provide recommendations for future urban planning.

5.2. Issues Related to the ULU Classification Approach

Firstly, numerous researchers highlight the limitations of medium-resolution Landsat imagery for ULU classification due to mixed pixels. Alternatively, high-resolution Google Earth imagery presents an opportunity for ULU classification through visual interpretation. However, use of Google Earth imagery has a limitation that precludes time series analysis due to the non-availability of multi-temporal imageries [39], which can be achieved using Landsat imagery. Thus, despite their limitations, the two freely available remote sensing data sets present a good opportunity for ULU classification, especially in a developing SSA city like Lusaka where expensive high-resolution satellite imagery cannot be easily obtained.

At the same time, using ULU parcels to separate ULU presented some issues. Initially, we considered using a fully automated system trained to detect parcels based on similarity and/or shape and size to classify our ULU classes, as recommended by [10]. However, the variance among parcels in the study area limited the use of this approach. For example, unplanned areas, especially in the UHDR class, lacked clearly defined road networks, which resulted in high variance among the generated parcels (see Figure 3a). Indeed, in some cases parcels were created through on-screen digitisation. Thus, we applied a semi-automated system by automatically assigning ULU attributes to parcels using the spatial ancillary data and thereafter systematically scrutinising and refining ULU parcels through visual interpretation of high-resolution Google Earth imagery. Nevertheless, the use of visual interpretation had issues of its own. Visual classification requires that researchers have expert prior knowledge of the study area [36]. In this study, our knowledge of the study area and the six ULU categories in terms of context, texture, size, location, and historical development [41] was extensive, thus reducing the possibility of misinterpretation. It is for this reason that we identify our approach as a somewhat expert-based approach. Another issue considered was the tendency of visual interpreters to generalise areas that are fragmented or composed of more than one ULU class within a parcel [42]. We successfully dealt with this issue by introducing the cadastral and land use data, which contained detailed information of the ULU attributes of the study area and thus reduced the potential for interrupters to ignore details among mixed ULU parcels. It is, however, important to note that the number of visual misinterpretations can also be determined by the classification scheme, the type, and the availability of ancillary data required, as well as the purpose of the study. In our ULU classification, for example, it was going to be very difficult to discriminate between unplanned and planned areas or commercial buildings and public institutional buildings located within the same area without detailed cadastral and land use data from the local planning office.

Overall, with the above issues considered, we were able to achieve our primary objective of classifying ULU in the complex urban landscape of Lusaka with acceptable accuracies. However, some limitations that might limit our approach from being applied in other urban areas should be considered. First, we recognise that detailed ancillary data, mainly cadastral and land use data, is often not available, especially in developing regions such as those in SSA countries. We also acknowledge that the general trend has involved the use of a fully automated urban LUC classification processes with a complex set of rules and that this might be more desirable. The framework presented is semi-automated and requires expert knowledge to scrutinise ULU within parcels. This can be very difficult in the absence of proper ancillary data and could be a drawback in cases where researchers are not familiar with the study area. Even so, it should be noted that not all automated complex processes will work in all conditions, and diversity in available approaches is essential [39]. Moreover, the variations in the level of complexity of urban LUC among different localities limits most methods from being applied under a different set of conditions [5]. Thus, exploring approaches that can work at local and/or regional scales remains imperative.

6. Conclusions

In this study, we presented an approach for classifying ULU in the developing SSA city of Lusaka. Taking into account the inherent challenges of ULU classification, including the complexity

of SSA urban areas and the resulting spectral confusion among ULU types, the limited availability and cost of high-resolution remote sensing data, as well as the limited applicability of available ULU classification methods, we developed a framework for integrating remote sensing and GIS techniques to classify ULU. We demonstrated that utilising more than one geospatial technique plus additional ancillary spatial data (i.e., road network, cadastral, and land use data), the challenges and limitations encountered when using freely available remote sensing datasets (i.e., Landsat and Google Earth imagery) can be overcome to an acceptable level. We successfully classified the study area into six ULU classes (i.e., unplanned high density residential areas; unplanned low density residential areas; planned medium/high density residential areas; planned low density residential areas; commercial and industrial areas; and public institutions and service areas) with high overall classification accuracy values (84.09% and 85.86%) and kappa coefficients (80.63% and 84.02%). The ULU maps produced in this study provide detailed information on the spatial-temporal patterns of ULU in the study area. In addition, the statistics provide an insight on the trends of ULU in Lusaka. For instance, throughout the study period (1990–2010), the statistics show that the growth of Lusaka has been dominated by informal/slum areas (i.e., UHDR) which have the highest population densities in the city and are mainly characterised by high poverty levels, unemployment, environmental degradation, and limited access to public services (health, education, water, and sanitation, etc.). Such information can be used by planning authorities to decide on the appropriate infrastructure development, provision of public services, as well as urban landscape management. The visualisation of the trends and patterns of ULU can also help urban planners and policy makers, including other concerned stakeholders (e.g., researchers), to analyse the city growth and provide recommendations for future urban development planning. This study also provides insights for ULU classification in complex urban landscapes of other SSA cities similar to Lusaka.

An important future research direction for this study is to investigate the potential for automating the process of ULU scrutiny within parcels. Perhaps a good place to start would be to consider models that can detect unplanned informal settlements within parcels from features, such as their physical attributes and spatial arrangement, in relation to the distribution of other ULU types.

Author Contributions: The corresponding author, Matamyo Simwanda, proposed the topic and spearheaded the design, data processing and analysis, and writing of the manuscript. Yuji Murayama helped in the design, research implementation, and analysis and writing of the manuscript.

Conflicts of Interest: The authors declare no conflicts of interest.

References

1. Barnsley, M.J.; Barr, S.L.; Hamid, A.; Muller, P.A.L.; Sadler, G.J.; Shepherd, J. Analytical tools to monitor urban areas. In *Geographical Information Handling—Research and Applications*; Mather, P.M., Ed.; John Wiley and Sons: Hoboken, NJ, USA, 1993; pp. 147–184.
2. Herold, M.; Scepan, J.; Clarke, K.C. The use of remote sensing and landscape metrics to describe structures and changes in urban land uses. *Environ. Plan. A* **2002**, *34*, 1443–1458. [CrossRef]
3. Stoler, J.; Daniels, D.; Weeks, J.R.; Stow, D.A.; Coulter, L.L.; Finch, B.K. Assessing the utility of satellite imagery with differing spatial resolutions for deriving proxy measures of slum presence in Accra, Ghana. *GISci. Remote Sens.* **2012**, *1*, 31–52. [CrossRef] [PubMed]
4. Barnsley, M.J.; Barr, S.L. Inferring urban land use from satellite sensor images using kernel-based spatial reclassification. *Photogramm. Eng. Remote Sens.* **1996**, *62*, 949–958.

5. Feyisa, G.L.; Meilby, H.; Darrel Jenerette, G.; Pauliet, S. Locally optimized separability enhancement indices for urban land cover mapping: Exploring thermal environmental consequences of rapid urbanization in Addis Ababa, Ethiopia. *Remote Sens. Environ.* **2016**, *175*, 14–31. [CrossRef]

6. Shaba, M.A.; Dikshit, O. Improvement of classification in urban areas by the use of textural features: The case study of Lucknow city, Uttar Pradesh. *Int. J. Remote Sens.* **2001**, *22*, 565–593. [CrossRef]

7. Myint, S.W.; Gober, P.; Brazel, A.; Grossman-Clarke, S.; Weng, Q. Per-pixel vs. object-based classification of urban land cover extraction using high spatial resolution imagery. *Remote Sens. Environ.* **2011**, *115*, 1145–1161. [CrossRef]

8. Salehi, M.; Sahebi, M.R.; Maghsoudi, Y. Improving the accuracy of urban land cover classification using Radarsat-2 PolSAR data. *IEEE J. Sel. Top. Appl. Earth Obs. Remote Sens.* **2014**, *7*, 1394–1401.

9. Harris, P.M.; Ventura, S.J. The integration of geographic data with remotely sensed imagery to improve classification in an urban area. *Photogramm. Eng. Remote Sens.* **1995**, *61*, 993–998.

10. Hu, T.; Yang, J.; Li, X.; Gong, P. Mapping Urban Land Use by using Landsat Images and Open Social Data. *Remote Sens.* **2016**, *8*, 151. [CrossRef]

11. Mesev, V. The use of census data in urban image classification. *Photogramm. Eng. Remote Sens.* **1998**, *64*, 431–436.

12. Lu, D.; Weng, Q. Use of impervious surface in urban land-use classification. *Remote Sens. Environ.* **2006**, *102*, 146–160. [CrossRef]

13. Mundia, C.N.; Aniya, M. Analysis of land use/cover changes and urban expansion of Nairobi city using remote sensing and GIS. *Int. J. Remote Sens.* **2005**, *26*, 2831–2849. [CrossRef]

14. Kamusoko, C.; Gamba, J.; Murakami, H. Monitoring urban spatial growth in Harare Metropolitan. *Adv. Remote Sens.* **2013**, *2*, 322–331. [CrossRef]

15. Gong, P.; Howarth, P.J. The Use of Structural Information for Improving Land-Cover Classification Accuracies at the Rural-Urban Fringe. *Photogramm. Eng. Remote Sens.* **1990**, *56*, 67–73.

16. Steinnocher, K. Integration of Spectral and Spatial Classification Methods for Building a Land-Use Model of Austria. *Int. Arch. Photogramm. Remote Sens.* **1996**, *31*, 841–846.

17. Van de Voorde, T.; Jacquet, W.; Canters, F. Mapping form and function in urban areas: An approach based on urban metrics and continuous impervious surface data. *Landsc. Urban Plan.* **2011**, *102*, 143–155. [CrossRef]

18. Lu, D.; Weng, Q. Spectral mixture analysis of the urban landscape in Indianapolis with Landsat ETM+ imagery. *Photogramm. Eng. Remote Sens.* **2004**, *70*, 1053–1062. [CrossRef]

19. Jensen, J.; Cowen, D. Remote sensing of urban suburban infrastructure and socio-economic attributes. *Photogramm. Eng. Remote Sens.* **1999**, *65*, 611–622.

20. Mudau, N.; Mhangara, P.; Gebreslasie, M. Monitoring urban growth around Rustenburg, South Africa, using SPOT 5. *S. Afr. J. Geomat.* **2014**, *3*, 185–196. [CrossRef]

21. Central Statistical Office (CSO). *2010 Census of Population and Housing*; Lusaka, Zambia, 2012. Available online: http://www.zamstats.gov.zm/report/Census/2010/National/2010%20Census%20of%20Population%20Summary%20Report.pdf (accessed on 20 January 2017).

22. Bhaskaran, S.; Paramananda, S.; Ramnarayan, M. Per-pixel and object-oriented classification methods for mapping urban features using Ikonos satellite data. *Appl. Geogr.* **2010**, *30*, 650–665. [CrossRef]

23. Aguirre-Gutiérrez, J.; Seijmonsbergen, A.C.; Duivenvoorden, J.F. Optimizing land cover classification accuracy for change detection, a combined pixel-based and object-based approach in a mountainous area in Mexico. *Appl. Geogr.* **2012**, *34*, 29–37. [CrossRef]

24. Li, X.; Meng, Q.; Gu, X.; Jancso, T.; Yu, T.; Wang, K.; Mavromatis, S. A hybrid method combining pixel-based and object-oriented methods and its application in Hungary using Chinese HJ-1 satellite images. *Int. J. Remote Sens.* **2013**, *34*, 4655–4668. [CrossRef]

25. Trimble. eCognition®Developer 9.0 User Guide, 2014. Available online: http://www.eCognition.com/ (accessed on 22 February 2015).

26. El-Kawy, O.A.; Rød, J.K.; Ismail, H.A.; Suliman, A.S. Land use and land cover change detection in the western Nile delta of Egypt using remote sensing data. *Appl. Geogr.* **2011**, *31*, 483–494. [CrossRef]

27. Congalton, R.G. A review of assessing the accuracy of classification of remotely sensed data. *Remote Sens. Environ.* **1991**, *37*, 34–46. [CrossRef]

28. Stefanov, W.L.; Ramsey, M.S.; Christensen, P.R. Monitoring urban land cover change: An expert system approach to land cover classification of semiarid to arid urban centers. *Remote Sens. Environ.* **2001**, *77*, 173–185. [CrossRef]

29. Hung, M.; Ridd, M.K. A subpixel classifier for urban land-cover mapping based on a maximum-li kelihood approach and expert system rules. *Photogramm. Eng. Remote Sens.* **2002**, *68*, 1173–1180.

30. Kahya, O.; Bayram, B.; Reis, S. Land cover classification with an expert system approach using Landsat ETM imagery: A case study of Trabzon. *Environ. Monit. Assess.* **2010**, *160*, 431–438. [CrossRef] [PubMed]

31. Liu, X.; Long, Y. Automated identification and characterization of parcels with OpenStreetMap and points of interest. *Environ. Plan. B Plan. Des.* **2016**, *43*, 341–360. [CrossRef]

32. Anderson, J.R.; Hardy, E.E.; Roach, J.T.; Witmer, R.E. *A Land Use and Land Cover Classification System for Use with Remote Sensor Data*; Geological Survey Professional Paper; USGS: Reston, VA, USA, 1976.

33. Pontius, R.G., Jr.; Malizia, N.R. Effect of Category Aggregation on Map Comparison. *Geogr. Inf. Sci.* **2004**, *3234*, 251–268.

34. Rocha, J.; Sousa, P.M.; Tenedório, J.A.; Encarnação, S. Land use/cover maps by RS and ancillary data integration in a GIS environment. Global developments in environmental earth orbservation from space. In Proceedings of the 25th EARSeL Symposium, Porto, Portugal, 6–11 June 2005; pp. 487–494.

35. Chang, C.; Ye, Z.; Huang, Q.; Wang, C. An integrative method for mapping urban land use change using geo-sensor data. In Proceedings of the 1st International ACM SIGSPATIAL Workshop on Smart Cities and Urban Analytics, Seattle, WA, USA, 3–6 November 2015; pp. 47–54.

36. Ghorbani, A.; Pakravan, M. Land use mapping using visual vs. digital image interpretation of TM and Google Earth derived imagery in Shrivan-Darasi watershed (Northwest of Iran). *Eur. J. Exp. Biol.* **2013**, *3*, 576–582.

37. Jaafari, S.; Nazarisamani, A. Comparison between land use/land cover mapping through Landsat and Google Earth imagery. *Am. J. Agric. Environ. Sci.* **2013**, *13*, 763–768.

38. Jacobson, A.; Cattau, M.; Riggio, J.; Petracca, L.; Fedak, D. Distribution and abundance of lions in northwest Tete Province, Mozambique. *Trop. Conserv. Sci.* **2013**, *6*, 87–107. [CrossRef]

39. Jacobson, A.; Dhanota, J.; Godfrey, J.; Jacobson, H.; Rossman, Z.; Stanish, A.; Walker, H.; Riggio, J. A novel approach to mapping land conversion using Google Earth with an application to East Africa. *Environ. Model. Softw.* **2015**, *72*, 1–9. [CrossRef]

40. Herold, M.; Liu, X.; Clarke, K.C. Spatial Metrics and Image Texture for Mapping Urban Land Use. *Photogramm. Eng. Remote Sens.* **2003**, *69*, 991–1001. [CrossRef]

41. King, R.B. Land cover mapping principles: A return to interpretation fundamentals. *Int. J. Remote Sens.* **2002**, *23*, 3525–3545. [CrossRef]

42. Puig, C.J.; Hyman, G.; Bolaños, S. Digital Classification vs. Visual Interpretation: A case study in humid tropical forests of the Peruvian Amazon. *Int. Cent. Trop. Agric.* 2002. Available online: https://www.researchgate.net/publication/237021820_Digital_Classification_vs_Visual_Interpretation_a_case_study_in_humid_tropical_forests_of_the_Peruvian_Amazon (accessed on 28 March 2017).